

The chemical evolution of subpopulations in the Carina dwarf spheroidal

A. Koch¹, M. Wilkinson², E.K. Grebel¹, D. Harbeck³, J. Kleyna⁴,
R. Wyse⁵, G. Gilmore² and W. Evans²

¹Astronomical Institute of the University of Basel, Venusstr. 7, 4102 Binningen, Switzerland
email:koch@astro.unibas.ch

²Institute of Astronomy, Cambridge University, Madingley Road, Cambridge CB3 0HA, UK

³University of California, Space Sciences Laboratory, 7 Gauss Way, Berkeley, CA 940720

⁴Institute for Astronomy, University of Hawaii, 260 Woodlawn Drive, Honolulu, HI 96822

⁵The John Hopkins University, 3701 San Martin Drive, Baltimore, MD 21218

Abstract. We present the observed metallicity distribution for 437 red giants in the Carina dwarf spheroidal (dSph) galaxy that was derived from FLAMES medium-resolution spectroscopy of the near-infrared Ca triplet (CaT). We find a mean [Fe/H] of -1.7 dex and a full spread in metallicities of at least one dex. Most of this width is due to the occurrence of three populations at different [Fe/H], which are likely to be related to the three star forming (SF) episodes that governed Carina's evolution and also correlate with peaks in the age-distribution. Both the lack of any correlation between stellar colour and metallicity and a comparison of the metallicities with chemical evolution models, which suggest a major role of infalling gas, contribute to the detailed understanding of Carina's evolutionary history. Moreover, we find a mild dependence of metallicity on radial location, reflected in a shift of the distribution's peak towards the metal poor end in the outer regions.

Keywords. galaxies: abundances, galaxies: evolution, galaxies: dwarf

1. Stellar populations in Carina

Photometric analyses of the faint Carina dSph have disclosed the presence of various stellar populations (e.g., Monelli *et al.* 2003), exhibiting a prominent old (>11 Gyr), intermediate-age (5–6 Gyr), and a young (3 Gyr) population. This implies that Carina must have undergone several SF episodes with at least three significant pulses. In apparent defiance of the resulting spread in ages, the galaxy's colour-magnitude diagram (CMD) features a remarkably narrow red giant branch (RGB). A reason for that can be a counteracting spread in metallicities, where metal rich, young stars have colours comparable to the older, more metal poor ones. Such an undesired age-metallicity degeneracy can be resolved if independent, accurate [Fe/H] measurements are available so that stellar ages as the remaining parameter can be obtained from isochrones. Moreover, the overall shape and possible spatial variations of the metallicity distribution functions (MDFs) themselves provide vital ingredients for analysing Carina's unusual SF history.

With the aim of studying the chemical *and* kinematical properties of Carina's separate populations we launched an ESO Large Programme. In this vein, spectroscopic observations of five fields in Carina were performed, comprising 1257 red giants out to the tidal radius, thus providing a wide spatial coverage and good number statistics. Our observations were performed during 23 nights with the multi-object spectrograph FLAMES at the VLT in medium-resolution mode (grating LR8), centered at the near-infrared CaT around 860 nm. For details on the data reduction and calibration see Koch *et al.*,

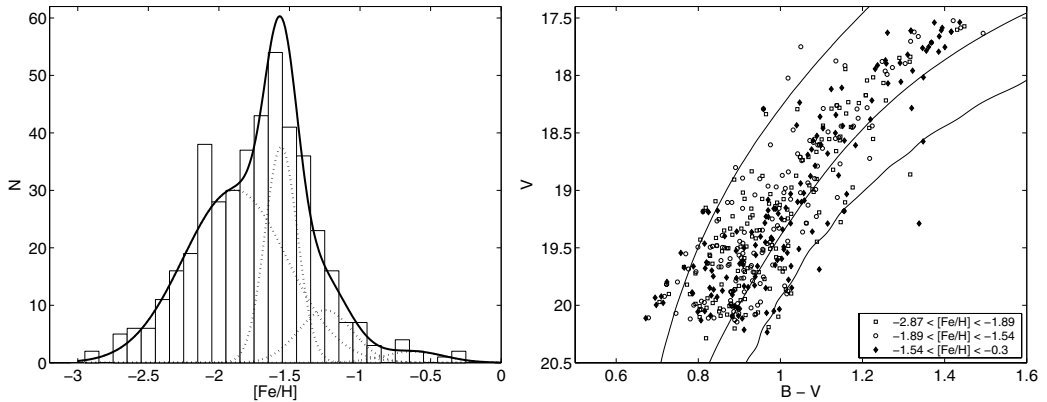


Figure 1. *Left panel:* MDF for our sample of red giants in Carina. Also indicated are the populations as revealed by a KMM-test (dotted lines) and the sum of these populations (solid). The *right panel* illustrates the distribution of metallicities across the RGB, where different symbols refer to three ranges of $[\text{Fe}/\text{H}]$. Solid lines indicate globular cluster fiducials from Sarajedini & Layden (1997): M 15 ($[\text{Fe}/\text{H}] = -2.17$), NGC 6752 (-1.54) and NGC 1851 (-1.29).

in preparation. Typical signal-to-noise (S/N) ratios for the spectra lie between 25 and 150 pixel^{-1} . Rejection of foreground stars could be achieved by iterative error-weighted Gaussian fits of the radial velocity distribution upon convergence, which yields a distinctive peak at 224 km s^{-1} with a respective dispersion of 7.5 km s^{-1} . This procedure (cutting at 3σ), after additional rejection of stars with too low a S/N to measure equivalent widths, left 437 radial velocity members to be analysed. Finally, metallicities were derived from the reduced equivalent width W' (Rutledge *et al.* 1997, Cole *et al.* 2004) of the CaT, which we calibrated against a common reference dataset of galactic globular clusters, obtained during the same observational runs.

2. Metallicity distributions

The resulting MDF for our 437 red giants is displayed in the left panel of Fig. 1. Its formal mean lies at an $[\text{Fe}/\text{H}]$ of -1.72 ± 0.01 dex, and the dispersion is $\sigma = 0.37$ dex, whereas the distribution implies that the full spread in $[\text{Fe}/\text{H}]$ is at least one dex. Considering this wide spread and the measurement uncertainties, this is well in agreement with the spectroscopic study of Smecker-Hane *et al.* (1999), who found a value of -1.99 ± 0.08 dex from a low number of stars, and also with the estimate of Rizzi *et al.* (2003) of -1.91 ± 0.18 dex as inferred from their CMDs after correction of age effects. The apparent presence of a secondary peak in the MDF at lower metallicities and the occurrence of three SF episodes in Carina led us to perform a KMM-test for multiple populations (cf. left panel of Fig. 1). As a result, four populations are preferred against the hypothesis of only two or three peaks and their significance versus a one-population model lies at a confidence of 98.1%. The major part of stars ($\sim 67\%$) in our sample has peak metallicities at -1.89 dex, whereas 21% of the targets can be assigned to a population around -1.56 dex. The remaining 12% form the more metal rich tail composed of peaks at -1.2 and -0.6 dex.

2.1. Absence of colour trends

A puzzling feature of Carina's CMD is the RGB, which is, in spite of the wide age range covered by the galaxy's stellar populations, remarkably narrow. However, the ever so wide observed spread in metallicities is able to explain this narrowness in terms of a counteraction of age versus metallicity in the sense that metal rich, young stars have colours

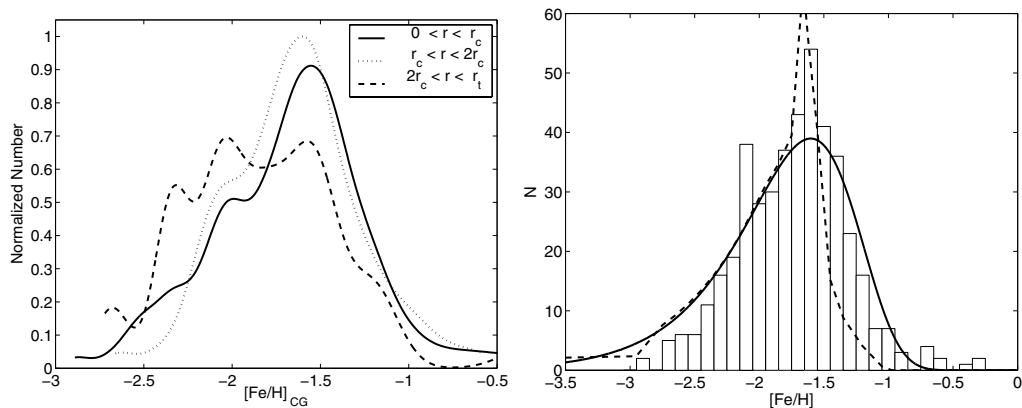


Figure 2. *Left:* Generalized MDFs after convolution with an error distribution for different radial bins in Carina. The *right* panel are overplots of the best-fit curve from a closed box model (solid line) and of a model from Lanfranchi & Matteucci (2004) on the observed MDF.

comparable to the older, more metal poor ones (Smecker-Hane *et al.* 1999). This in fact confirms that a complex mixture of stellar populations as in Carina does not necessarily contradict the RGB’s narrowness. As the right panel of Fig. 1 implies, there is no apparent trend of $[\text{Fe}/\text{H}]$ with the colour of the red giants – different metallicity subgroups are equally widely spread across the whole width of the RGB. Thus producing metal rich and metal poor giants at the same location in the CMD requires the more metal poor stars to be also older and, vice versa, that the metal rich stars at the respective locus tend to have younger ages. Hence there seems to be an indication of an age-metallicity relation of some kind in Carina, although this is not immediately obvious from the CMD.

2.2. Presence of radial trends

The different stellar populations in Carina have often photometrically been shown to take different spatial distributions, where the intermediate age red clump stars are clearly concentrated towards the center compared to the old HB (see Harbeck *et al.* 2001). Such a radial trend seems to be a common feature among the dSphs of the Local Group. In order to assess whether such a gradient is also reflected in our spectroscopic metallicity sample, we plot in Fig. 2 (left panel) the error-weighted MDFs for three radial bins, each with a width of approximately one core radius ($8''.8$). The distribution from the central region shows evidence of the different populations, reflected in the occurrence of peaks at several metallicities. When proceeding outwards to the middle annulus, the peak of the entire MDF is shifted by ca. 0.1-0.2 dex towards the metal poor end, whereas there is an increasing contribution from the secondary peak at ~ -2.1 dex. Finally, the outermost bin shows an increasing tendency towards the metal poor tail of the distribution, with a similar contribution from all the different peaks. In addition to this spatial separation of stellar populations in terms of their chemical properties, there is also evidence of kinematic substructure, see Wilkinson – this proceedings.

2.3. Models of chemical evolution

Overplotted on the observed MDF in Fig. 2 (right) is the curve for a best-fit simple closed box model. This model is able to roughly reproduce the metal poor peak and the metal rich tail of the distribution. Likewise, a more sophisticated model from Lanfranchi & Matteucci (2004), which incorporates the infall and outflow of material from the galaxy and is characterised by a remarkably low SF efficiency and a high wind rate, predicts the

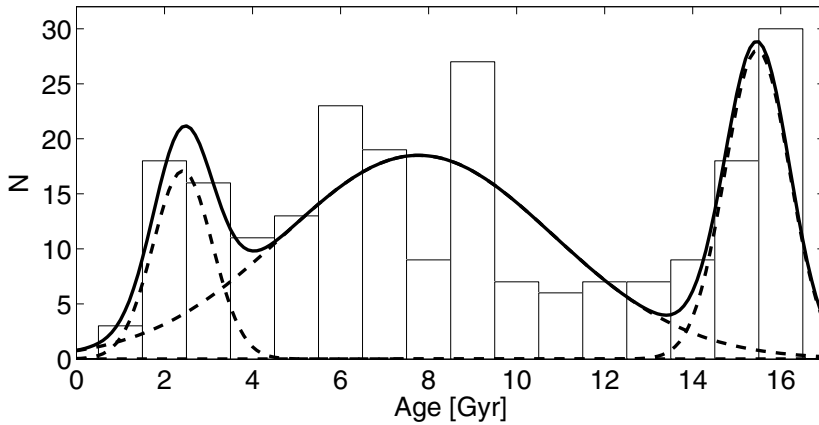


Figure 3. Preliminary age distribution of stars in Carina, together with separate fits of the underlying populations from a KMM-test.

metal poor peak and the slow decline towards the metal poor end of the distribution[†]. However, all such models tend to overpredict the number of extremely metal poor stars, which we do not see in the observations. This is in fact comparable to the (solar) G-dwarf problem. The general failure of a simple closed-box assumption points to the fact that Carina cannot be taken as a closed system and it must be rather considered as likely that the star forming bursts were triggered by the infall of (pre-enriched) gas.

2.4. Stellar ages

With the accurate $[\text{Fe}/\text{H}]$ measurements on hand stellar ages could be estimated from isochrone fits to each star's location in the CMD. The *preliminary* distribution shown in Fig. 3 is drawn from a set of Y^2 -isochrones with no α -enhancement. Again, there is strong evidence of at least three underlying populations, where a KMM-test reveals a young population at 2.5 Gyr (with 13% of all stars), a rather old population at ca. 15 Gyr (23%) and the major part (64%) of the giants at intermediate ages around 7.8 Gyr. Both the young and old population appear to be rather narrow, with a formal width of 0.8 Gyr, whereas the dominant intermediate age population spans a range of at least 3 Gyr.

3. Conclusions

The analysis of a large number of spectroscopic metallicities in the Local Group dSph Carina has revealed the presence of detailed substructure in this particular galaxy, which is most likely related to the occurrence of extended SF bursts. Both the MDF itself and also the age distribution show three distinct populations, whereas the radial variation of metallicities and comparison with chemical evolutionary models argue in favour of a dominant role of infalling gas onto the galaxy. Sophistication of the isochrone grids and completion of the ongoing analysis of multi-object high-resolution spectroscopy will then deepen the detailed understanding of Carina's evolutionary history.

[†] Note, however, that the latter model was not fit to our data, but we rather overplotted the curve from literature, which the authors labelled their “best-fit model”.

References

- Cole, A. *et al.* 2004, *MNRAS* 347, 367
Lanfranchi, G. & Matteucci, F. 2004, *MNRAS* 351, 1338
Monelli, M. *et al.* 2003, *AJ* 126, 218
Rizzi, L., Held, E.V., Bertelli, G. & Saviane, I. 2003, *ApJ* 589, L85
Rutledge, G.A., Hesser, J.E. & Stetson, P.B. 1997, *PASP* 109, 907
Sarajedini, A & Layden, A. 2003, *AJ* 113, 264
Smecker-Hane, T.A. *et al.* 1999, *ASP* 192, 159

Discussion

ZAGGIA: What is the impact of your radial velocity errors on the chemical abundance calculations?

KOCH: Our median measurement error is 1.2 km s^{-1} . Any possible inclusion of one or two remaining non-members will *not* alter the conclusions from the metallicity distributions.

